Case Study

From Basic Particle Gradation Parameters to Water Retention Curves and Tensile Strength of Unsaturated Granular Soils

Ji-Peng Wang[1]; Bertrand François[2]; and Pierre Lambert[3]

Abstract: The long-debated effective stress definition of unsaturated soils is believed to be correlated to suction, the degree of saturation, and the less mentioned interfacial areas. The tensile strength of unsaturated soils is directly associated with the effective stress definition in theory, and it is also crucial in engineering practices. For unsaturated soils, the relationship between suction and degree of saturation can be described as the water retention curve (WRC), which is related to the pore-size distribution. In the meanwhile, the air–water interfacial area is also regarded as a function of the degree of saturation, and parameters of the function are determined by the soil's pore structures. For granular soils, the pore-size distribution is usually in a unimodal shape and, therefore, the strength properties can also be related to the particle gradation parameters. In this study, a preliminary estimation method is proposed for the tensile strength of unsaturated sandy soils based on basic particle gradation parameters. In this method, with basic physical features considered, WRC is estimated from a characteristic grain diameter (d_{60}) and the coefficient of uniformity (C_u). The function to determine the air–water interfacial area is also formulated by soil gradation parameters of the mean grain-size (d_{50}), the coefficient of uniformity (C_u), and the void ratio. The proposed tensile strength estimation is compared with experimental measurements on sandy soils, which shows fair agreement, especially for the conventional split plate method. Qualitatively, the tensile strength is inversely proportional to soil mean grain-size and is increased with particle-size polydispersity.
DOI: 10.1061/(ASCE)GM.1943-5622.0001677. © *2020 American Society of Civil Engineers*.

Author keywords: Unsaturated soil; Particle-size distribution; Water retention curve; Tensile Strength; Interface area.

Downloaded from ascelibrary.org by Shandong University on 06/27/20. Copyright ASCE. For personal use only; all rights reserved.

Introduction

The water retention curve (WRC) or the soil-water characteristic curve (SWCC), which is the relationship between the degree of saturation and suction, is an important hydraulic property for unsaturated soils. It also affects the soil mechanical behaviors such as strength coupled with effective stress formulations. Water retention behavior is related to particle-size distribution (PSD), soil texture, and relative density (Gupta and Larson 1979; Saxton et al. 1986; Vereecken et al. 1989), which is usually referred to as pedotransfer functions (PTFs) (Bouma 1989). For sandy soil, its void ratio variation is relatively small, and its pore-size distribution usually has a single peak, which is associated with its PSD (Feia et al. 2014). Thus, the WRC may be predicted from PSD (Wang et al. 2017b), which will save experiment time and cost.

On the other hand, among different strength property measurements, tensile strength is a significant value which should be investigated in different engineering problems. For example, the soil cracking phenomena, which is affected by tensile strength, is vital for the development of slope sliding, road embankment instability, earth dam failure, etc. (Vahedifard et al. 2016; Xu et al. 2011). Moreover, tensile strength is one of the most fundamental and direct evidences for the effective stress definition of unsaturated soils. The cohesive effect in unsaturated soils is mainly induced by two aspects. One is from the negative pore-water pressure (suction), which is intrinsically associated with water retention behavior. Another important origin is from the interfacial areas with the action of surface tension. In the present day, the interfacial area effect attracts more and more attention in the investigation of unsaturated soil mechanics (Gray et al. 2009; Nikooee et al. 2013). As we mentioned before, water retention behavior of a clean granular soil can be estimated from its particle-size distribution. Recently, Yin and Vanapalli (2018) raised a new model to predict the tensile strength of unsaturated soils in which the interface effect is included. They proposed that the air–water interfacial area could be related to the soil uniformity coefficient C_u. This means that, together with the pedotransfer function, the total tensile strength of an unsaturated granular soil with various degree of saturation could be preliminarily estimated from its particle-size distribution parameters. A new tensile strength model based on these is thereafter emerged.

We proposed an estimation method to study the relationship between PSD and WRC for sandy soils through a semiphysical and semistatistical way. The classic van Genuchten's model (van Genuchten 1980) is adopted to describe the WRC. Dimensional analysis is applied to clarify the key parameters. A monosized granular packing and an extremely polydisperse packing are considered to enhance the physical basis. Then, a couple of new pedotransfer functions are proposed by using basic parameters of d_{60} and C_u. Furthermore, we also compare the estimation of the interfacial area (Yin and Vanapalli 2018) with our X-ray CT measurements, which coincide with each other. Then, by coupling the proposed PTFs with the recent effective stress definitions (Lu et al. 2010; Nikooee et al. 2013) and also including the interfacial area effects (Yin and Vanapalli 2018), a new model to estimate the tensile strength of sandy soils is derived. Justifications of this model are implemented by comparing the estimated WRCs and tensile strength characteristic curves with experimental measurements of

[1]School of Civil Engineering, Shandong Univ., Jingshi Rd. 17922, Jinan 250061, China (corresponding author). ORCID: https://orcid.org/0000-0001-7082-8864. Emails: ji-peng.wang@sdu.edu.cn; ji-peng.wang@outlook.com

[2]Building Architecture and Town Planning Dept. (BATir), Univ. Libre de Bruxelles, Avenue F.D. Roosevelt 50, CP 194/2, Brussels 1050, Belgium.

[3]TIPs Dept., Univ. Libre de Bruxelles, Avenue F.D. Roosevelt 50, CP 165/56, Brussels 1050, Belgium.

Note. This manuscript was submitted on January 31, 2019; approved on November 5, 2019; published online on March 25, 2020. Discussion period open until August 25, 2020; separate discussions must be submitted for individual papers. This paper is part of the ***International Journal of Geomechanics***, © ASCE, ISSN 1532-3641.

various granular materials in literature. Furthermore, a qualitative investigation is also carried out by studying the particle-size effect on tensile strength parametrically. It helps to understand the fundamental relationship between particle-size and strength properties from two key aspects: the mean grain-size and the particle-size polydispersity. It should be noted that the proposed method in this study is only valid for sandy soils which have single peak pore-size distributions. For clay or soil with a certain amount of fine content, the pore structure may be more complicated; for example, it could be a dual pore structure. In that case, the estimation methods for water retention curve and strength properties in this study may not be valid.

Estimation of Water Retention Curves from Particle-Size Distribution

The Water Retention Curve in van Genuchten's Model

With the increase of soil suction, the degree of saturation starts to decrease when it reaches the air entry value (AEV) and air bubbles enter the water phase. Then the degree of saturation reduces significantly with the suction increase and both water and air phases become continuous (see Fig. 1 where large pores start to drain while smaller pores are still filled with water). When the suction value is very high, the water phase exists as isolated water bridges and adsorption layers. Further change of suction has little further influence on the degree of saturation. This state is called the residual state. The definition of the effective degree of saturation is usually adopted to characterize the water retention behavior as

$$S_e = \frac{\theta - \theta_r}{\theta_s - \theta_r} = \frac{S_r - S_r^r}{1 - S_r^r} \tag{1}$$

where θ, θ_s, and θ_r = water content, saturated water content, and residual water content, respectively; S_r and S_r^r = degree of saturation and residual degree of saturation. In the classic van Genuchten's model (van Genuchten 1980), the effective degree of saturation is expressed as

$$S_e = \left(1 + \left(\frac{s}{\alpha_{vg}}\right)^{n_{vg}}\right)^{(1/n_{vg})-1} \tag{2}$$

where s = soil suction; α_{vg} = a parameter related to air entry value; and n_{vg} = a parameter related to WRC slope.

Estimation of van Genuchten's Model Parameters by d_{60} and C_u

Wang et al. (2017b) proposed two pedotransfer equations to predict the WRC by estimating the van Genuchten's model parameters from grain-size distribution. The equations are semiphysical and semiempirical. In this section, we reintroduce the basic ideas briefly.

In geotechnical engineering, d_{10}, d_{30}, and d_{60} (particle sizes at 10%, 30%, and 60% passing by weight) are three important particle sizes in describing soil gradation (Terzaghi et al. 1996). With the coefficient of uniformity ($C_u = d_{60}/d_{10}$), the coefficient of curvature ($C_c = d_{30}^2/(d_{60}d_{10})$), and a measure of mean particle size, the shape of PSD can be determined. In this model, d_{60} is used to quantify the mean grain-size. Dimensional analysis, after Buckingham's Pi theorem (Buckingham 1914), is employed to clarify the controlling parameters in the unsaturated granular system. In WRC, the effective degree of saturation (S_e) relies on the PSD, suction, and also the water surface tension value (noted as γ). The variation of void ratio for sandy soil is assumed to be small. Here, $S_e[-]$ can then be expressed as a function of variables of $C_u[-]$, $C_c[-]$, $d_{60}[\mathrm{L}]$, $s[\mathrm{ML}-1T-2;]$, and $\gamma[\mathrm{MT}-2;]$, where means dimensionless and L, M, and T represent length, mass, and time units, respectively. Then after dimensional analysis

$$S_e = f(C_u, C_c, d_{60}, s, \gamma) = f'\left(C_u, C_c, \frac{sd_{60}}{\gamma}\right) \tag{3}$$

By neglecting the effect of C_c, the relationship can be simplified as

$$S_e \approx f''\left(C_u, \frac{sd_{60}}{\gamma}\right) \tag{4}$$

The van Genuchten's equation can also be rewritten by normalized suction ($s^* = sd_{60}/\gamma$) and normalized $\alpha_{vg}(\alpha_{vg}^* = \alpha_{vg}d_{60}/\gamma)$ as

$$S_e = \left(1 + \left(\frac{s^*}{\alpha_{vg}^*}\right)^{n_{vg}}\right)^{(1/n_{vg})-1} \tag{5}$$

In Eq. (4), there are only two controlling parameters, s^* and C_u. In Eq. (5), in addition to s^*, there are two more parameters n_{vg} and α_{vg}^*. Normally, n_{vg} is believed to be related to coefficient of uniformity (C_u). Therefore, the normalized parameter $\alpha_{vg}^* = \alpha_{vg}d_{60}/\gamma$ is either related to C_u or is a constant.

To make the analysis more applicable, two extreme conditions are considered. The first case is a monosized granular material, thus the coefficient of uniformity $C_u = 1$. If the particles are

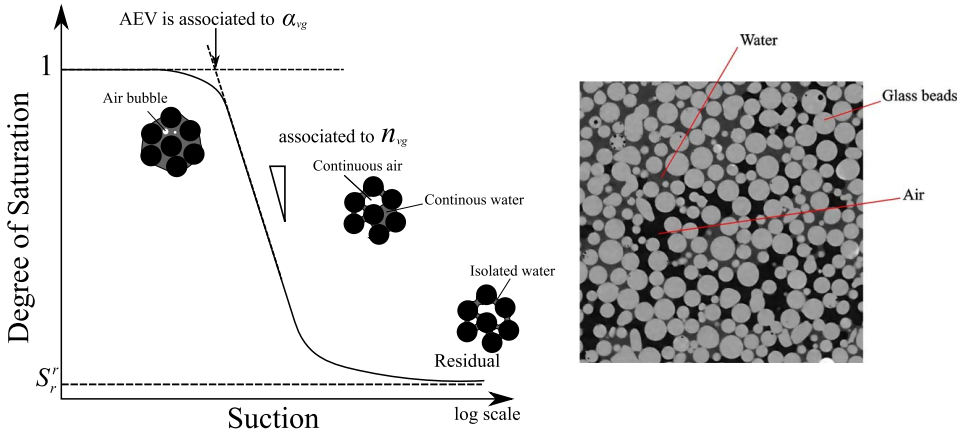

Fig. 1. Water retention curve and a cross-section of an unsaturated granular material by X-ray tomography.

Int. J. Geomech., 2020, 20(6): 05020003

Downloaded from ascelibrary.org by Shandong University on 06/27/20. Copyright ASCE. For personal use only; all rights reserved.

assumed to be spheres, pore size in the granular medium will also be uniform. This means when suction reaches the air entry value all pores should start to drain. The slope of the WRC is nearly infinite ($n_{vg} \to \infty$). Another scenario is that C_u is very high. This means that large pores are filled with finer particles and the soil is very difficult to desaturate. Therefore, the slope of the WRC will be a rather flat shape. The minimum value of parameter n_{vg} will be reduced to approach 1.

The empirical relationship is based on 70 sandy soils from the UNSODA database (Leij et al. 1996) and eight granular materials (four glass beads and four sands with different particle-size distributions) tested by Wang et al. (2017b). The 70 sandy soils from UNSODA have clear and continuous PSD and reached the residual state with high suctions. The eight tested granular materials have relatively low C_u values. In Fig. 2(a), the best-fitted n_{vg} parameters of the 78 samples are plotted against $\log_{10} C_u$. When the material is nearly monosized, C_u approaches to 1 and the parameter n_{vg} tends to be infinite. When the grain-size is highly dispersed (C_u is a very high value), the parameter n_{vg} decreases to about 1. The following equation is proposed to represent the n and $\log_{10} C_u$ relationship:

$$n_{vg} = \frac{C_1}{\log_{10} C_u} + 1 \tag{6}$$

where C_1 is a constant; and $C_1 \approx 1.07$ by a regression analysis of 78 soils.

In the dimensional analysis, the normalized parameter $\alpha_{vg}^* = \alpha_{vg} d_{60}/\gamma$ is believed to be either related to C_u or to be a constant. It is found that the normalized α_{vg} is not obviously influenced by C_u. Therefore, it is assumed that $\alpha_{vg} d_{60}/\gamma$ is approximately a constant C_2 and the parameter α_{vg} can be approximated from d_{60} as

$$\alpha_{vg} = \frac{C_2 \gamma}{d_{60}} \tag{7}$$

Fig. 2(b) demonstrates the correlation between α_{vg} and d_{60}. Here, C_2 is fitted to be 12.07 by the 78 materials.

Wang et al. (2017b) compared the above relationship with other pedotransfer functions in literature and found that the new equations have a better performance. They also validate the above two equations on sandy soils beyond the analyzed database and found it is widely valid for clean sandy soils with little clayey or silty fines. Therefore, Eqs. (6) and (7) will be employed in the later sections to estimate the tensile strength property.

Estimation of Tensile Strength

Effective Stress of Unsaturated Granular Soils

The effective stress definition is the cornerstone of modern soil mechanics after Terzaghi (1943). For unsaturated soils, the first and the most classic effective stress formulation is the Bishop's effective stress (Bishop and Blight 1963) which is expressed as

$$\sigma'_{ij} = (\sigma_{ij} - u_a \delta_{ij}) + \chi(u_a - u_w)\delta_{ij} \tag{8}$$

where u_a = pore-air pressure; u_w = pore-water pressure; δ_{ij} = Kronecker delta; and χ is called the "Bishop's coefficient," which is believed to be relevant to the degree of saturation (or suction). The pressure difference between air and water, $u_a - u_w$, is matric suction which is also associated with the degree of saturation through the water retention behavior (WRC).

Some authors simply approximate the Bishop's coefficient χ as the degree of saturation (Nuth and Laloui 2008; Schrefler 1984). The Bishop's coefficient can also be estimated as an exponential relationship with the normalized suction (Khalili and Khabbaz 1998). More recently, χ is suggested to be only associated with the free water in the microstructure (Alonso et al. 2010). However, the effect of air–water surface tension has not been considered in the previous work.

Lu et al. (2010) proposed a suction stress characteristic curve to unify the effective stress definitions of saturated and unsaturated soils. They express the effective stress as

$$\sigma'_{ij} = (\sigma_{ij} - u_a \delta_{ij}) - \sigma^s_{ij} \tag{9}$$

where σ^s = suction stress. Based on a virtual work principle, the suction stress term can be derived, and the interfacial energy is included in the expression

$$\sigma^s_{ij} = -S_e(u_a - u_w)\delta_{ij} - \sum_i \gamma_i \frac{\partial A_i}{\partial V}\delta_{ij} \tag{10}$$

where S_e = effective degree of saturation; V = volume; γ_i = interfacial free energy of the ith interface; and A_i = interfacial surface area of the ith interface. Although the interfacial area effect exists in the formula derivation, the second term is ignored in their experimental validation as the interfacial areas are difficult to be measured. Nikooee et al. (2013) also verified the above effective stress expression by a thermodynamic approach. The complete effective stress of unsaturated

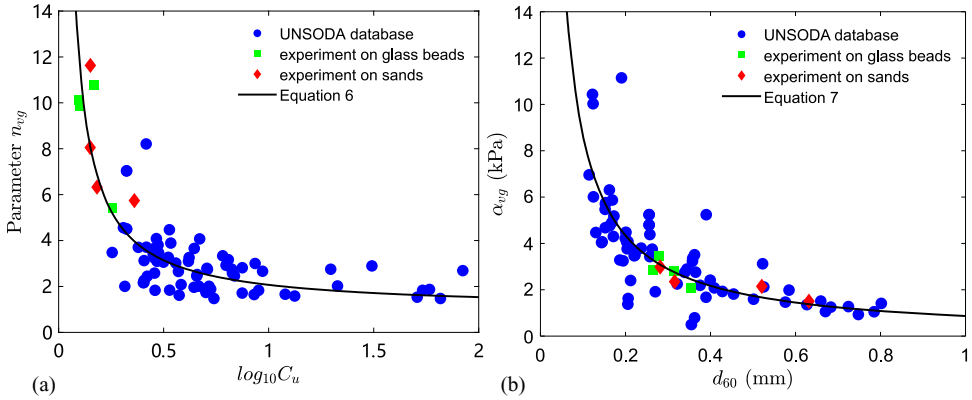

Fig. 2. Predicted van Genuchten's model parameters and measured values: (a) relationship between n_{vg} and C_u; and (b) relationship between α_{vg} and d_{60}.

Downloaded from ascelibrary.org by Shandong University on 06/27/20. Copyright ASCE. For personal use only; all rights reserved.

soil can be formulated by simplifying the last term as

$$\sigma'_{ij} = (\sigma_{ij} - u_a\delta_{ij}) + S_e(u_a - u_w)\delta_{ij} + \gamma a_{aw}\delta_{ij} \quad (11)$$

where γ = air–water surface tension (0.072 N/m is taken in this study); and a_{aw} = the specific air–water interfacial area (the air–water interfacial area per total volume).

Here it should be noted that when the degree of saturation is within the residual state, the suction term is 0 (taking $S_e = 0$ when $0 < S_r < S_r^r$). However, the surface tension term may still contribute to the soil strength. It has been observed that with a tiny amount of water, the strength of granular materials can be significantly increased by pendular water bridges (Scheel et al. 2008; Wang et al. 2017c, 2018). Theoretically, the water pressure and air pressure terms contribute to the material strength together with the air–water surface tension or interfacial area effect. However, in the pendular regime, the water phase is not a continuous phase. The local meniscus curvatures or pressure may not be the same, as both convex and concave menisci exist among granular particles (Lourenço et al. 2012). Therefore, it gives justifications to ignore the pressure effect while the surface tension effect is retained.

Estimation of Air–Water Interfacial Area

It is usually not easy to quantify the interfacial area from experiments. Although it becomes possible by using high-resolution X-ray CT (Culligan et al. 2006; Wang et al. 2019; Willson et al. 2012), the measurement is still relatively expensive and time-consuming. For granular soils with a continuous particle-size distribution, the pore-size distribution has a unimodal shape. The air–water interfacial area in the material is believed to be related not only to the degree of saturation but also to grain-size. Based on simple water bridge and cubic unit pore-cell assumptions, Likos and Jaafar (2013) proposed a model to estimate the interfacial area from the pore-size distribution. As pore-size distribution is associated with particle-size distribution, estimating the interfacial area from particle-size distribution will be more applicable to engineering practice. Rumpf (1961) and Schubert et al. (1975) indicated that the tensile strength induced by surface tension could be inversely proportional to void ratio and mean grain-size in addition to the effect of degree of saturation. Following their spirit and considering the position of the peak strength, Yin and Vanapalli (2018) proposed a semiempirical equation to estimate the air–water interfacial area for cohesionless granular soils. We may rewrite the equation as

$$a_{aw} = \eta_s \frac{\pi}{e d_{50}} S_r^{\lambda_s}(1 - S_r) \quad (12)$$

where η_s = magnitude of the interfacial area; λ_s = degree of saturation with the peak interfacial area; e = void ratio; and d_{50} = mean grain diameter. After an analysis of a number of cohesionless soils, Yin and Vanapalli (2018) also indicates that the parameter η_s should also be related to the grain-size uniformity parameter C_u and they proposed a linear relationship as

$$\eta_s = k_s C_u \quad (13)$$

They suggest that $k_s \approx 0.73$ based on a regression analysis on 10 soils. Here it should be noted that in Eq. (12), we used the degree of saturation term S_r instead of the effective degree of saturation S_e. This is because, as introduced in the previous section, the surface tension effect (or the interfacial area effect) is significant within the pendular state through water bridges between particles.

We may also verify the relationship in Eqs. (12) and (13) by comparing the model prediction with X-ray CT measurements. Following Wang et al. (2019), high-resolution X-ray CT technique can be employed to measure interfacial areas of wet granular materials.

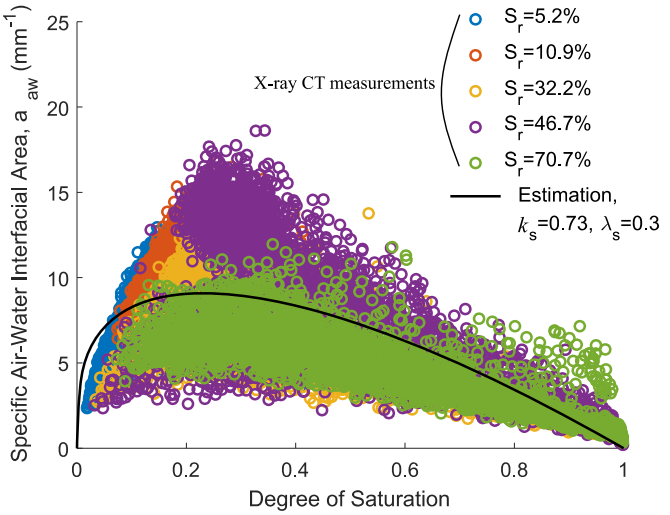

Fig. 3. X-ray CT measured specific interfacial area and equation estimation.

Glass beads with grain diameters ranging from 0.2 to 0.4 mm are used for this study. Five samples with different degree of saturation are prepared and scanned on the micro-CT facility HECTOR in Gent University (Masschaele et al. 2013). The void ratio of the five glass bead samples is around 0.61. The mean particle size d_{50} is 0.3 mm and the uniformity coefficient C_u is about 1.47. Resolution of the obtained images from X-ray CT is about 5.85 μm per pixel. Then the images are reconstructed and segmented into three phases in the three-dimensional (3D) space. A Representative Volume Element (RVE)-based analysis method is adopted to measure the local degree of saturation and interfacial areas. That is to say, a sample is meshed into cubic subelements based on which the measurement is implemented. The elements are in cubic shape with 110 pixels in width (two times of the mean grain diameter), which is the minimum size that can bear a stable pore structure. Due to the nature of water distribution heterogeneity, the local elements should cover the full range of degree of saturation and should also include all possible interfacial area values statistically.

Fig. 3 presents the relationship between the local degree of saturation and local air–water interfacial areas for all the elements in the five samples (the global degree of saturation is presented in the legend). It can be seen that the overall saturation and interfacial area relationship follows a rise and fall trend. The maximum air–water interfacial area value is around 0.3 degree of saturation. We also plot the predicted value of Eq. (12) to have a verification of the model. Here, $\lambda_s = 0.3$ is taken and we keep the suggestion of $k_s = 0.73$ by Yin and Vanapalli (2018). It can be seen that the predicted line falls within the full range of the X-ray measurements (the clouded data). This means that the estimation model by Yin and Vanapalli (2018) has a fair accuracy. We will use the model of Yin and Vanapalli (2018) and keep their model parameter values in the following analysis.

Relating WRC and Interface Area with Tensile Strength

To calculate the strength properties of unsaturated sandy soils, the failure criterion should be determined first. In this study, the Mohr–Coulomb failure criterion is adopted to model the material strength. For sandy soils, there is no cohesion when the material is completely dry or fully saturated. When it is partially saturated, its cohesion is due to the suction effect and air–water surface tension. Incorporating the effective stress definition in Eq. (11) and

Downloaded from ascelibrary.org by Shandong University on 06/27/20. Copyright ASCE. For personal use only; all rights reserved.

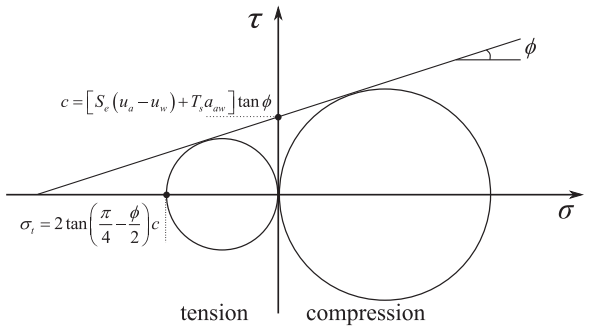

Fig. 4. Mohr–Coulomb type failure and uniaxial tensile strength.

considering cohesion is the intercept between the Mohr–Coulomb failure line, cohesion can be formulated as

$$c = [S_e(u_a - u_w) + \gamma a_{aw}]\tan\phi \tag{14}$$

where ϕ = the friction angle of the material. After Richefeu et al. (2006), the friction angle is assumed not to be obviously affected by water content for dry and partially saturated granular soils.

The tensile strength is estimated based on the assumption that the linear Mohr–Coulomb failure criterion is also valid in the tensile process. For soil mechanics, we use the positive sign to represent stress in compression and the negative signs for tensile stress. For a uniaxial tensile test without confining stress, its first principle stress is 0. By drawing a Mohr circle crossing the point of origin and tangential to the Mohr–Coulomb failure envelope, the uniaxial tensile strength can be obtained. According to the geometry in Fig. 4, the uniaxial tensile strength has a relation with cohesion as

$$\sigma_t = 2\tan\left(\frac{\pi}{4} - \frac{\phi}{2}\right)\cdot c = \frac{2\cos\phi}{1+\sin\phi}\cdot c \tag{15}$$

By rewriting van Genuchten's model in Eq. (5) as a function of the effective degree of saturation, suction in the cohesion term can be expressed as

$$s = u_a - u_w = \alpha_{vg}(S_e^{n_{vg}/(1-n_{vg})} - 1)^{1/n_{vg}} \tag{16}$$

It can be substituted into the cohesion and tensile strength equations. The estimation model in Eqs. (6) and (7) can also be substituted in the tensile strength formulation. Then, finally, we can obtain the following equation to estimate the tensile strength:

$$\sigma_t = 2\tan\phi\tan\left(\frac{\pi}{4}+\frac{\phi}{2}\right)\left\{\frac{C_2\gamma}{d_{60}}S_e[S_e^{-((C_1+\log_{10}C_u)/C_1)} - 1]^{\log_{10}C_u/(C_1+\log_{10}C_u)} + \gamma k_s C_u\frac{\pi}{ed_{50}}S_r^{\lambda_s}(1-S_r)\right\} \tag{17}$$

with $S_e = [(S_r - S_r^r)/(1 - S_r^r)]$ being kept in mind. In this equation, ϕ, γ, C_1, C_2, k_s, and λ_s are material constants; ϕ is the friction angle which can be measured from the dry sand; γ is water–air surface tension (for distilled water it is 0.072 N/m at 20°C); C_1, C_2, k_s, and λ_s are independent of soil gradation. Based on regression analysis, C_1 and C_2 are suggested to be 1.07 and 12.07, respectively, for all sandy soils within the applicable range. Here, $k_s = 0.73$ and $\lambda_s = 0.3$ are taken by following Yin and Vanapalli (2018) (these constants are summarized in Table 1). Therefore, the uniaxial tensile strength can be estimated by grain-size parameters of d_{50}, d_{60}, C_u, and void ratio e with a given degree of saturation.

It should be noted that the hysteresis effect in the WRC is not considered in this estimation method. In the literature, some authors consider that the friction angle depends on the stress level. For example, the friction angle under relatively low normal stress is regarded as a much larger value than the normal friction angle (Likos et al. 2010; Lu et al. 2009). However, from our perspective, there are two unsolved points. The first is that the systematic measurement error may be more significant for very low stress conditions with a traditional testing apparatus. The second point is that more direct evidence is required to confirm the friction angle for materials in tension. Therefore, we still keep the conventional friction angle concept for this study. It will demonstrate a fair prediction in the later section.

Model Verification and Discussion on Particle-Size Effect

This section will demonstrate the performance of the prediction model by comparing the estimated WRC and tensile strength with the experimental measurements in literature. Some qualitative analysis will also be provided to investigate the particle-size effect on material strength.

Table 1. Summary of model constants

Parameter	Value
γ (N/m)	0.072
C_1	1.07
C_2	12.07
k_s	0.73
λ_s	0.3

WRC and Tensile Tests with Constant Suction

As the model does not consider the hydraulic history effect, water retention tests following the main drying path and suction controlled tensile tests are more suitable for the model validation. Schubert (1972) investigated the tensile strength of a series of granular materials including both limestone aggregates and glass balls. A split plate apparatus conducted the tests with the negative water pressure controlled by a U-shape manometer (Schubert 1975). The tensile force was applied from the horizontal direction. As air pressure in this apparatus is 0 (connected to the atmosphere), the measured head difference in the U-shape manometer represents the suction.

Grain-size of the tested limestone aggregates ranges from about 0.03 to 0.2 mm. The mean grain diameter d_{50} is about 0.071 mm, d_{60} is about 0.087 mm, and the uniformity coefficient C_u is about 1.64. Soil gradation and other model parameters are summarized in Table 2. Fig. 5 compared the experimental results of WRC and tensile strength with the model estimated results. In the prediction of WRC, the residual degree of saturation S_r^r is 0.2. It can be seen that using particle-size parameters to estimate the van Genutchten's model through Eqs. (6) and (7) gives a good agreement with the experimental measurements. For the tensile strength, the maximum tensile strength appears at around 92% of saturation. It also has a second peak around 10% to 20% of degree of saturation

Downloaded from ascelibrary.org by Shandong University on 06/27/20. Copyright ASCE. For personal use only; all rights reserved.

Table 2. Soil gradation and soil parameters of the studied soils

Granular soil name	Testing method	d_{50} (mm)	d_{60} (mm)	C_u	e	$\varnothing(^\circ)$	S_r^r
Limestone aggregates	Constant suction, split plate	0.071	0.087	1.64	0.71	40	0.2
Glass balls	Constant suction, split plate	0.15	0.15	1.35	0.59	30	0.05
Ottawa sand	Constant water content, split plate	0.21	0.24	2	0.65	36	0.17
Silica sand	Constant water content, split plate	0.42	0.46	1.96	0.65	36	0
Perth medium sand	Constant water content, tilt tube	0.45	0.47	1.5	0.67	30	0.1
Perth fine sand	Constant water content, tilt tube	0.17	0.18	1.5	0.82	30	0.05
Perth silty sand	Constant water content, tilt tube	0.1	0.12	1.8	0.82	30	0.02

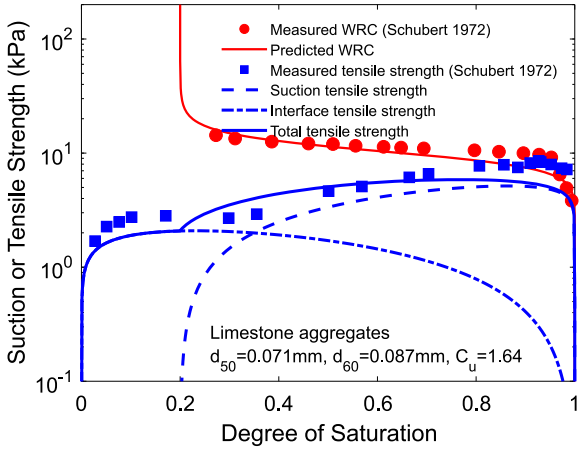

Fig. 5. Model estimation and measured data of limestone aggregates.

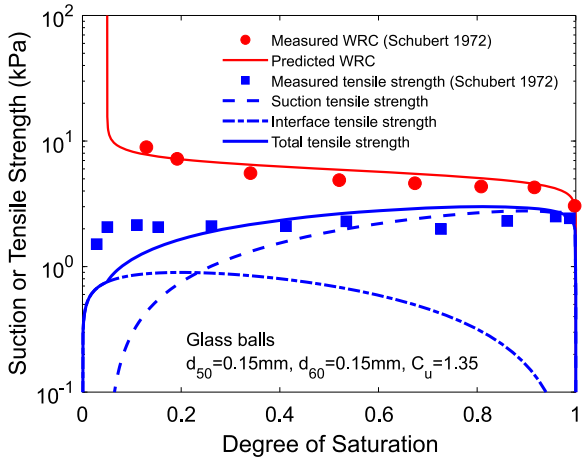

Fig. 6. Model estimation and measured data of glass balls.

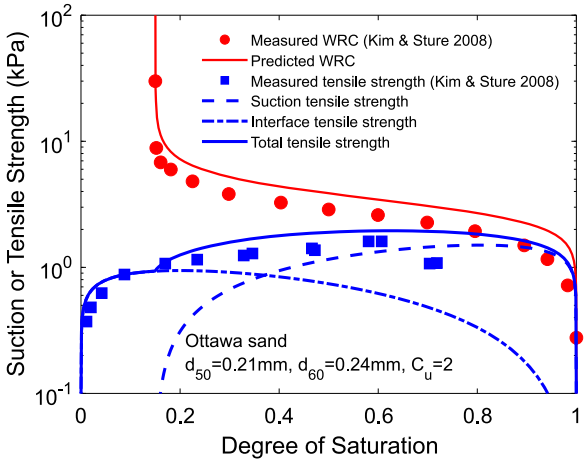

Fig. 7. Model estimation and measured data of Ottawa sand F75.

within the pendular state. The tested material has a void ratio of 0.71. In our estimation, we used a typical friction angle of 40° for crushed limestone aggregates. Then, based on the particle-size parameters, the uniaxial tensile strength can also be predicted by Eq. (17). The estimation fairly agrees with the tested results. It also has a bimodal shape with one peak in the pendular regime and the maximum peak appears in the high degree of saturation range. It represents that the tensile strength within the pendular state is mainly contributed by the interfacial area term but the maximum tensile strength of this material is mainly due to the suction effect. The maximum tensile strength of the estimation is slightly lower than the measurements, which is due to the underestimation of suction in the high saturation range.

Schubert (1972) also tested the WRC and tensile strength of glass balls. Results of a glass balls sample with particle size ranging from 0.07 to 0.2 mm are used for model validation. The void ratio of the sample is 0.59. Here, d_{50} and d_{60} are about 0.15 mm and the uniformity coefficient C_u is 1.53. By taking $S_r^r = 0.05$, it can be seen from Fig. 6 that Eqs. (6) and (7) give a very prediction on water retention behavior compared to experimental results. The internal friction angle of glass balls is around 30° (Richefeu et al. 2006). Then, based on the given particle-size distribution, the tensile strength is also calculated by Eq. (17). The estimated curve agrees with the tested results generally.

WRC and Tensile Tests with Constant Water Content

In literature, the number of suction-controlled tensile tests is limited. There are some water-content-controlled tensile strength tests, which can be used to compare with the proposed estimation method. Water retention behaviors of the tested materials may also validate the proposed pedotransfer functions in Eqs. (6) and (7).

Kim and Sture (2008) measured both the water retention behavior and the tensile strength of an Ottawa silica sand (F-75). The sand was produced by the Ottawa Silica Company. It has a mean size of 0.22 mm, its d_{60} is around 0.24 mm and the coefficient of uniformity C_u is 2. The sample was prepared at a certain void ratio and mixed with a certain amount of water. The tensile test apparatus was adopted from Perkins (1991). The tensile force was applied horizontally on a static sample. Here, we use the results of the clean Ottawa sand with a void ratio of 0.65 to do the comparison. The authors also tested the water retention curve of this sand, which also gives the opportunity to validate our water retention estimation. In Fig. 7, the measured WRC and tensile strength data are compared with model predictions. For WRC, the residual state degree of saturation is about 0.17. It can be observed that our estimation coincides with the measured values in drying path in trend. It has a slight overestimation in air entry value, which could be related to void ratio variation. By applying the internal angle of friction as 36°

Downloaded from ascelibrary.org by Shandong University on 06/27/20. Copyright ASCE. For personal use only; all rights reserved.

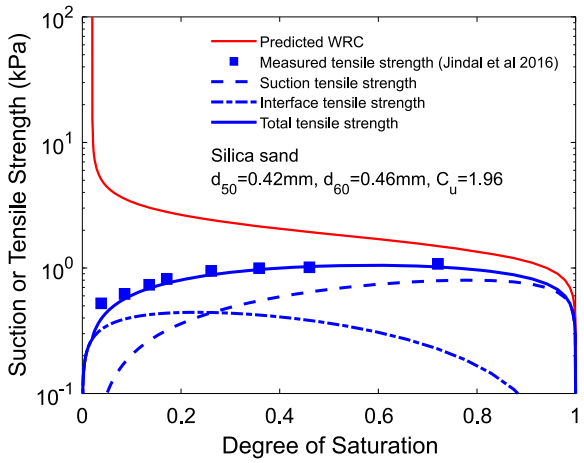

Fig. 8. Model estimation and measured data of a silica sand.

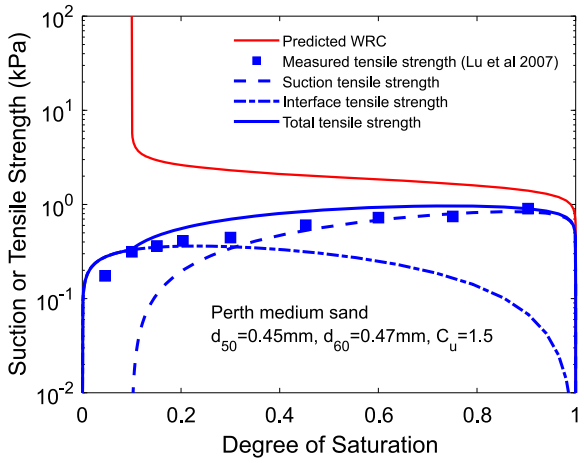

Fig. 9. Model estimation and measured data of a Perth medium sand.

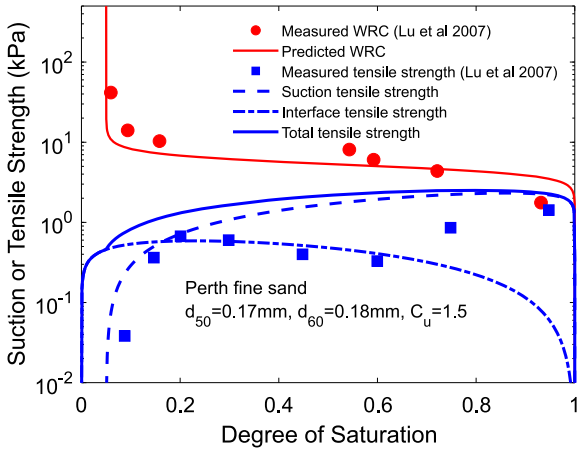

Fig. 10. Model estimation and measured data of a Perth fine sand.

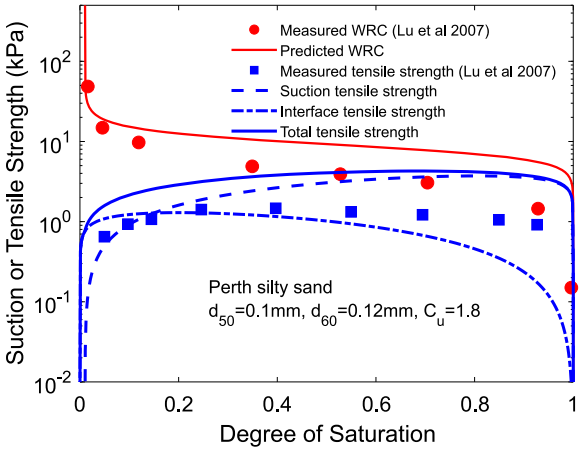

Fig. 11. Model estimation and measured data of a Perth silty sand.

for Ottawa sands (Baltodano-Goulding 2006), the estimated tensile strength also has a high accuracy comparing with the measured tensile strength. Its performance in the pendular state is even better. The maximum strength in the test is similar to the estimation. The model somehow overestimates the strength when $S_r > 0.7$, however, the measured results in this range are limited.

Jindal et al. (2016) used a similar testing method as Kim and Sture (2008) to measure the tensile strength of a silica sand. The tested silica sand was obtained from Sil Industrial Minerals, AB, Canada. The mean particle size d_{50} is about 0.42 mm, its d_{60} is 0.46 mm, and the coefficient of uniformity C_u is 1.96. Unfortunately, the WRC is not available for this material. The compared sand has a void ratio of 0.65 and the internal friction angle can be regarded as the same as Ottawa sand. By taking $S_r^r \approx 0$, we can still estimate the water retention behavior as well as its tensile strength characteristics from the equations introduced earlier. As can be seen in Fig. 8, it has very high accuracy in predicting the tensile strength characteristic curve.

Furthermore, Lu et al. (2007) also tested the tensile strength properties of different Perth sands. They used a different testing device. In their tests, the tensile strength was not directly measured by applying tensile forces. They prepared the sample in two halves of a cylindrical tube and then tilted the tube with the upper half being fixed until failure, then the tensile strength was calculated based on the tilting angle and the weight of the lower half.

A medium sand, a fine sand, and a silty sand were tested by the device. The soil gradation parameters, void ratio, friction angle, and residual degree of saturation of the studied soils are summarized in Table 2. The typical friction angle of Perth sands is around 30°. Then the measured tensile strength can be compared with the model estimation. Fig. 9 presents the comparison of the Perth medium sand. The WRC is not available, but we can take the residual degree of saturation as 0.1, which is a typical value for medium sands. It shows that the estimation represents a similar trend of the tensile strength characteristic curve. It reasonably predicts the maximum strength around 90% of saturation. Fig. 10 demonstrates the measured results of Perth fine sand, in which the WRC is also measured. It can be seen that the model prediction of WRC agrees well with the experimental measurements. However, there is an apparent overestimation in tensile strength. In Fig. 11, the measured data of Perth silty sand is compared with the model estimations. The estimation presents the trend of the measured data, but it overestimates the suction value and the tensile strength at the same degree of saturation. We should keep in mind that the tested method is different from the previous split plate method and the hydraulic history of the tested materials is unknown. The comparisons from Figs. 5 to 9 already prove that the proposed model could be a useful preliminary estimation method of WRC and tensile strength from basic particle gradation parameters.

Downloaded from ascelibrary.org by Shandong University on 06/27/20. Copyright ASCE. For personal use only; all rights reserved.

Qualitative Discussions of Particle-Size Effect on Tensile Strength

We may also have a qualitative investigation of the particle-size effect on tensile strength of granular soils, including the suction induced tensile strength term and the air–water interface tensile strength term. The soil gradation effect mainly has two aspects, one is the mean grain-size effect, and another one is the polydispersity effect in grain-size. Based on the proposed estimation model in Eq. (17), the two types of tensile strength can be estimated respectively based on the two terms in the bracket.

The air–water interfacial area (surface tension) induced tensile strength is related to grain-size from three parameters. The first one is the magnitude parameter η_s which is related to the uniformity parameter C_u according to Eq. (13). The second one is the mean grain-size d_{50} in the estimation model. The last one is the parameter void ratio, which is indirectly related to particle-size distribution. This is because, based on an empirical equation by Vukovic and Soro (1992), porosity of a granular soil (which can be replaced by void ratio as $e/(1+e)$) roughly has the following relationship with the uniformity coefficient C_u:

$$\frac{e}{1+e} = a(1 + b^{C_u}) \tag{18}$$

where a and b are constants. This relationship is reasonable as with a wider particle-size distribution, soil pores can be more easily filled by finer particles. It does not consider the void ratio variation for a same soil, but it gives the possibility to discuss the strength based on grain-size distribution qualitatively. Based on a study of 431 granular soils, $a = 0.2$ and $b = 0.93$ can be taken (Wang et al. 2017a). Fig. 12 represents the mean grain-size effect and the particle-size polydispersity effect on the tensile strength of the interfacial area term (angle of internal friction is assumed to be 30°). It can be seen that with the same particle-size uniformity, finer soils have higher interface-induced tensile strength. In the meanwhile, with the same mean particle diameter, a soil with higher uniformity coefficient has stronger tensile strength contributed by interfacial areas.

Furthermore, the effect of particle-size distribution on suction can also be investigated based on the predicted WRC and Eq. (17) (only taking the first term in the bracket). As d_{50} and d_{60} usually have similar values, we take $d_{50} \approx d_{60}$ to simplify the parametric study. Residual degree of saturation S_r^r is approximated as 0.1. In Fig. 13, effects of mean grain-size and uniformity are analyzed. With the same uniformity coefficient, a finer mean grain-size means a larger air entry value, which shifts the WRC. Therefore, the suction-induced tensile strength is inversely proportional to the mean grain-size. The degree of saturation of the maximum suction induced strength is not changed if C_u is the same. On the other hand, for soils with the same mean particle size, suction-induced tensile strength is stronger with a higher particle-size polydispersity. Due to the change of the slope of WRC, the maximum suction induced strength appears at a lower degree of saturation when C_u is larger.

Then the total tensile strength is obtained by summing the interface-induced tensile strength and the suction-induced tensile strength (Fig. 14). Similarly, with the same C_u, the maximum tensile strength is inversely proportional to the soil mean diameter. In the meanwhile, for soils with a same mean size, a wider

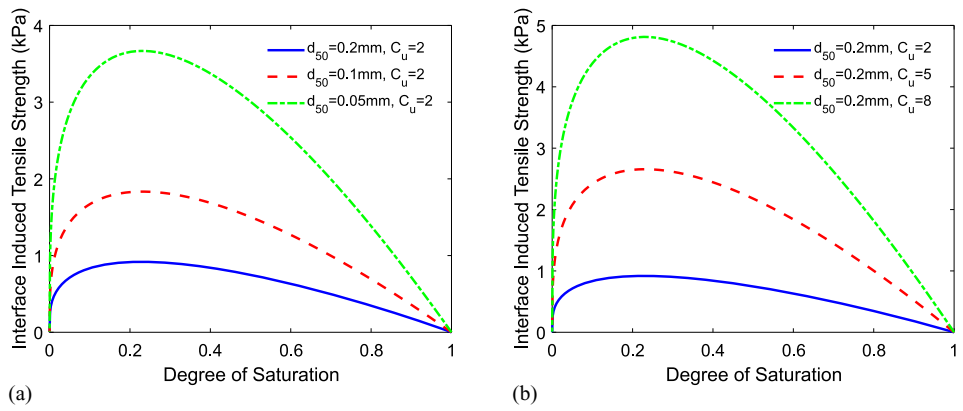

Fig. 12. Particle-size effect on tensile strength induced by air–water interface: (a) mean particle-size effect; and (b) grain-size polydispersity effect.

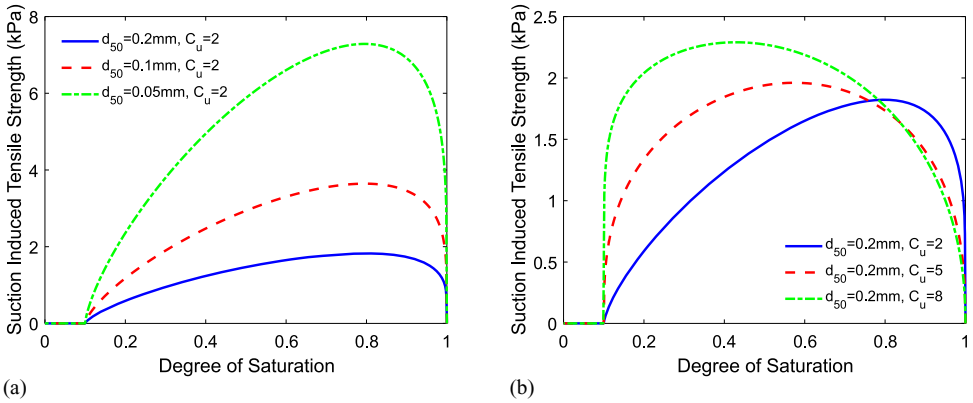

Fig. 13. Particle-size effect on tensile strength induced by suction: (a) mean particle-size effect; and (b) grain-size polydispersity effect.

Downloaded from ascelibrary.org by Shandong University on 06/27/20. Copyright ASCE. For personal use only; all rights reserved.

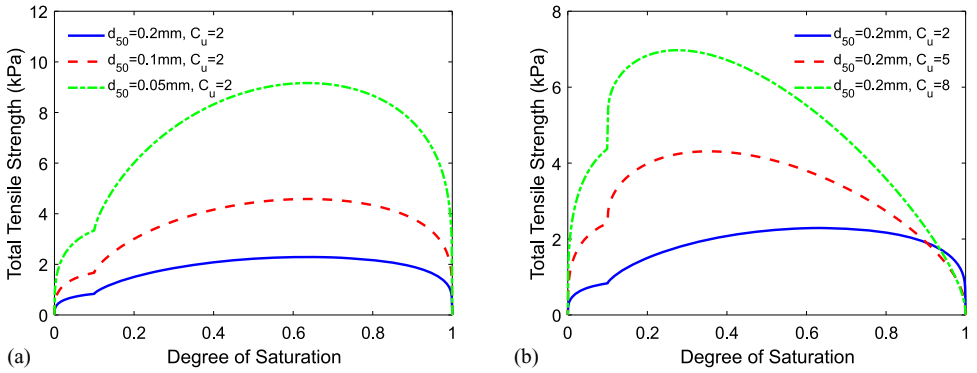

Fig. 14. Particle-size effect on total tensile strength: (a) mean particle-size effect; and (b) grain-size polydispersity effect.

particle-size distribution will lead the soil to have a higher maximum tensile strength and the soil can reach the maximum strength at a relatively lower degree of saturation.

Conclusions

Basic soil gradation parameters of d_{60} and C_u are employed to estimate the WRCs of unsaturated granular soils. Two extreme scenarios are considered to quantify the monosized material and the highly polydisperse sand, which enhances physical features to the statistical approach. A couple of semiempirical equations are proposed to estimate van Genuchten's model parameters which describes the WRC behavior of granular soils. The air entry value is inversely proportional to d_{60}. The WRC slope is inversely proportional to logarithmic C_u.

A recent effective stress definition, which accounts for the air–water interfacial area effect, is employed to couple with the proposed WRC prediction, which gives the possibility to estimate strength properties from particle-size distribution. Equations to estimate tensile strength are then derived based on the new pedotransfer functions and a recent approximation equation (Yin and Vanapalli 2018) on the air–water interfacial area. The estimated air–water interfacial area is compared with our experimental measurements by using high-resolution X-ray CT. It shows that the estimated curve is within the upper and lower boundaries of the measured data for the full range of degree of saturation. Therefore, it validates the referred interfacial area estimation.

The model estimation is then verified by experimental measurements of various granular soils in literature. Water retention behaviors are also compared with the model estimation if testing data is available. It shows that the estimation method generally agrees well with the tested results. It also indicates that the proposed model has a higher estimation accuracy for tensile tests using the conventional split plate method. A qualitative investigation of particle-size distribution effect on tensile strength is also carried out based on parametric studies. It demonstrates that both the suction-induced and interface-induced tensile strength terms are stronger for finer granular soil or soils with higher particle-size polydispersity. A wider particle-size distribution will also lead the maximum strength to appear at a relatively lower degree of saturation.

Data Availability Statement

All data and models used in this study are presented in the paper. The Matlab codes generated for figure plotting are available from the corresponding author.

Acknowledgments

The first author appreciates financial supports of National Natural Science Foundation of China (Grant No. 51909139) and Taishan Scholar Program of Shandong Province, China (Award No. tsqn201812009).

References

Alonso, E. E., J.-M. Pereira, J. Vaunat, and S. Olivella. 2010. "A microstructurally based effective stress for unsaturated soils." *Géotechnique* 60 (12): 913–925.

Baltodano-Goulding, R. 2006. "Tensile strength, shear strength, and effective stress for unsaturated sand." Ph.D. thesis, Dept. of Civil Engineering, Univ. of Missouri.

Bishop, A. W., and G. E. Blight. 1963. "Some aspects of effective stress in saturated and partly saturated soils." *Géotechnique* 13 (3): 177–197.

Bouma, J. 1989. "Using soil survey data for quantitative land evaluation." *Vol. 9 of Advances in soil science*, edited by B. A. Stewart, 177–213. New York: Springer.

Buckingham, E. 1914. "On physically similar systems; illustrations of the use of dimensional equations." *Phys. Rev.* 4 (4): 345–376.

Culligan, K. A., D. Wildenschild, B. S. B. Christensen, W. G. Gray, and M. L. Rivers. 2006. "Pore-scale characteristics of multiphase flow in porous media: A comparison of air–water and oil–water experiments." *Adv. Water Resour.* 29 (2): 227–238.

Feia, S., S. Ghabezloo, J. F. Bruchon, J. Sulem, J. Canou, and J. C. Dupla. 2014. "Experimental evaluation of the pore-access size distribution of sands." *Geotech. Test. J.* 37 (4): 20130126.

Gray, W. G., B. A. Schrefler, and F. Pesavento. 2009. "The solid phase stress tensor in porous media mechanics and the Hill–Mandel condition." *J. Mech. Phys. Solids* 57 (3): 539–554.

Gupta, S. C., and W. E. Larson. 1979. "Estimating soil water retention characteristics from particle size distribution, organic matter percent, and bulk density." *Water Resour. Res.* 15 (6): 1633–1635.

Jindal, P., J. Sharma, and R. Bashir. 2016. "Effect of pore-water surface tension on tensile strength of unsaturated sand." *Indian Geotech. J.* 46 (3): 276–290.

Khalili, N., and M. H. Khabbaz. 1998. "A unique relationship for χ for the determination of the shear strength of unsaturated soils." *Géotechnique* 48 (5): 681–687.

Kim, T.-H., and S. Sture. 2008. "Capillary-induced tensile strength in unsaturated sands." *Can. Geotech. J.* 45 (5): 726–737.

Leij, F. J., W. J. Alves, M. T. van Genuchten, and J. R. Williams. 1996. *The UNSODA unsaturated soil hydraulic database: User's manual*. Washington, DC: National Risk Management Research Laboratory, Office of Research and Development, US Environmental Protection Agency.

Likos, W. J., and R. Jaafar. 2013. "Pore-scale model for water retention and fluid partitioning of partially saturated granular soil." *J. Geotech.*

Downloaded from ascelibrary.org by Shandong University on 06/27/20. Copyright ASCE. For personal use only; all rights reserved.

Geoenviron. Eng. 139 (5): 724–737. https://doi.org/10.1061/(ASCE)GT.1943-5606.0000811.
Likos, W. J., A. Wayllace, J. Godt, and N. Lu. 2010. "Modified direct shear apparatus for unsaturated sands at low suction and stress." *Geotech. Test. J.* 33 (4): 1–13.
Lourenço, S. D. N., D. Galliposli, C. E. Augarde, D. G. Toll, P. C. Fisher, and A. Congreve. 2012. "Formation and evolution of water menisci in unsaturated granular media." *Géotechnique* 62 (3): 193–199.
Lu, N., J. W. Godt, and D. T. Wu. 2010. "A closed-form equation for effective stress in unsaturated soil." *Water Resour. Res.* 46 (5): W05515.
Lu, N., T.-H. Kim, S. Sture, and W. J. Likos. 2009. "Tensile strength of unsaturated sand." *J. Eng. Mech.* 135 (12): 1410–1419. https://doi.org/10.1061/(ASCE)EM.1943-7889.0000054.
Lu, N., B. Wu, and C. P. Tan. 2007. "Tensile strength characteristics of unsaturated sands." *J. Geotech. Geoenviron. Eng.* 133 (2): 144–154. https://doi.org/10.1061/(ASCE)1090-0241(2007)133:2(144).
Masschaele, B., M. Dierick, D. Van Loo, M. N. Boone, L. Brabant, E. Pauwels, V. Cnudde, and L. Van Hoorebeke. 2013. "HECTOR: A 240 kV micro-CT setup optimized for research." *J. Phys. Conf. Ser.* 463 (1): 012012.
Nikooee, E., G. Habibagahi, S. M. Hassanizadeh, and A. Ghahramani. 2013. "Effective stress in unsaturated soils: A thermodynamic approach based on the interfacial energy and hydromechanical coupling." *Transp. Porous Media* 96 (2): 369–396.
Nuth, M., and L. Laloui. 2008. "Effective stress concept in unsaturated soils: Clarification and validation of a unified framework." *Int. J. Numer. Anal. Methods Geomech.* 32 (7): 771–801.
Perkins, S. W. 1991. *Modeling of regolith structure interaction in extraterrestrial constructed facilities*. Boulder, CO: Univ. of Colorado.
Richefeu, V., M. El Youssoufi, and F. Radjaï. 2006. "Shear strength properties of wet granular materials." *Phys. Rev. E* 73 (5): 051304.
Rumpf, H. 1961. "The strength of granules and agglomerate." In *Agglomeration*, edited by W. Knepper, 379–414. New York: Wiley Interscience.
Saxton, K. E., W. J. Rawls, J. S. Romberger, and R. I. Papendick. 1986. "Estimating generalized soil-water characteristics from texture." *Soil Sci. Soc. Am. J.* 50 (4): 1031.
Scheel, M., R. Seemann, M. Brinkmann, M. Di Michiel, A. Sheppard, B. Breidenbach, and S. Herminghaus. 2008. "Morphological clues to wet granular pile stability." *Nat. Mater.* 7 (3): 189–193.
Schrefler, B. 1984. "The finite element method in soil consolidation (with applications to surface subsidence)." Ph.D. thesis, Dept. of Civil Engineering, Univ. College of Swansea.
Schubert, H. 1972. "Untersuchungen zur ermittlung von kapillardruck und Zug- festigkeit yon feuchten HauFwerken aus kSrnigen stoffen." Ph.D. thesis, Institut fur Mechanisehe Verfahrenstechnik, Univ. of Karlsruhe.
Schubert, H. 1975. "Tensile strength of agglomerates." *Powder Technol.* 11 (2): 107–119.
Schubert, H., W. Herrmann, and H. Rumpf. 1975. "Deformation behaviour of agglomerates under tensile stress." *Powder Technol.* 11 (2): 121–131.
Terzaghi, K. 1943. *Theoretical soil mechanics*. New York: John Wiley & Sons.
Terzaghi, K., R. Peck, and G. Mesri. 1996. *Soil mechanics in engineering practice*. New York: John Wiley & Sons.
Vahedifard, F., D. Leshchinsky, K. Mortezaei, and N. Lu. 2016. "Effective stress-based limit-equilibrium analysis for homogeneous unsaturated slopes." *Int. J. Geomech.* 16 (6): D4016003. https://doi.org/10.1061/(ASCE)GM.1943-5622.0000554.
van Genuchten, M. T. 1980. "A closed-form equation for predicting the hydraulic conductivity of unsaturated soils." *Soil Sci. Soc. Am. J.* 44 (5): 892–898.
Vereecken, H., J. Maes, J. Feyen, and P. Darius. 1989. "Estimating the soil moisture retention characteristic from texture, bulk density, and carbon content." *Soil Sci.* 148 (6): 389–403.
Vukovic, M., and A. Soro. 1992. *Determination of hydraulic conductivity of porous media from grain-size composition*. Littleton, CO: Water Resources Publications.
Wang, J.-P., B. François, and P. Lambert. 2017a. "Equations for hydraulic conductivity estimation from particle size distribution: A dimensional analysis." *Water Resour. Res.* 53 (9): 8127–8134.
Wang, J.-P., N. Hu, B. François, and P. Lambert. 2017b. "Estimating water retention curves and strength properties of unsaturated sandy soils from basic soil gradation parameters." *Water Resour. Res.* 53 (7): 6069–6088.
Wang, J.-P., P. Lambert, T. De Kock, V. Cnudde, and B. François. 2019. "Investigation of the effect of specific interfacial area on strength of unsaturated granular materials by X-ray tomography." *Acta Geotech.* 14: 1545–1559.
Wang, J.-P., X. Li, and H.-S. Yu. 2017c. "Stress–force–fabric relationship for unsaturated granular materials in pendular states." *J. Eng. Mech.* 143 (9): 04017068. https://doi.org/10.1061/(ASCE)EM.1943-7889.0001283.
Wang, J.-P., X. Li, and H.-S. Yu. 2018. "A micro–macro investigation of the capillary strengthening effect in wet granular materials." *Acta Geotech.* 13 (3): 513–533.
Willson, C. S., N. Lu, and W. J. Likos. 2012. "Quantification of grain, pore, and fluid microstructure of unsaturated sand from X-Ray computed tomography images." *Geotech. Test. J.* 35 (6): 20120075.
Xu, L., F. C. Dai, L. G. Tham, X. B. Tu, H. Min, Y. F. Zhou, C. X. Wu, and K. Xu. 2011. "Field testing of irrigation effects on the stability of a cliff edge in loess, North-west China." *Eng. Geol.* 120 (1): 10–17.
Yin, P., and S. K. Vanapalli. 2018. "Model for predicting tensile strength of unsaturated cohesionless soils." *Can. Geotech. J.* 21 (1): 1–21.

Downloaded from ascelibrary.org by Shandong University on 06/27/20. Copyright ASCE. For personal use only; all rights reserved.